

Search for light-to-heavy quark flavor changing neutral currents in $\nu_\mu N$ and $\bar{\nu}_\mu N$ scattering at the Tevatron

A. Alton, T. Adams, T. Bolton, J. Goldman, M. Goncharov, D. Naples*

Kansas State University, Manhattan, KS, 66506

R. A. Johnson, M. Vakili,[†] N. Suwonjandee

University of Cincinnati, Cincinnati, OH, 45221

J. Conrad, B. T. Fleming, J. Formaggio, J. H. Kim,[§] S. Koutsoliotas,[‡] C. McNulty,

A. Romosan,** M. H. Shaevitz, P. Spentzouris,^{††} E. G. Stern, A. Vaitaitis,

E. D. Zimmerman

Columbia University, New York, NY, 10027

R. H. Bernstein, L. Bugel, M. J. Lamm, W. Marsh, P. Nienaber,^{‡‡} J. Yu

Fermi National Accelerator Laboratory, Batavia, IL, 60510

L. de Barbaro, D. Buchholz, H. Schellman, G. P. Zeller

Northwestern University, Evanston, IL, 60208

*Present Address: University of Pittsburgh, Pittsburgh, PA , 15260

[†]Present Address: Texas A&M University, College Station, TX, 77843

[§]Present Address: University of California, Irvine, CA, 92697

[‡]Present Address: Bucknell University, Lewisburg, PA, 17837

**Present Address: University of California, Berkeley, CA, 94720

^{††}Present Address: Fermi National Laboratory, Batavia, IL, 60510

^{‡‡}Present Address: Marquette University, Milwaukee, WI, 53201

J. Brau, R. B. Drucker, R. Frey, D. Mason

University of Oregon, Eugene, OR, 97403

S. Avvakumov, P. de Barbaro, A. Bodek, H. Budd, D. A. Harris,^{††} K. S. McFarland,

W. K. Sakumoto, U. K. Yang

University of Rochester, Rochester, NY, 14627

Version 3.0.0

(November 21, 2018)

Abstract

We report on a search for flavor-changing neutral-currents (FCNC) in the production of heavy quarks in deep inelastic $\nu_\mu N$ and $\bar{\nu}_\mu N$ scattering by the NuTeV experiment at the Fermilab Tevatron. This measurement, made possible by the high-purity NuTeV sign-selected beams, probes for FCNC in heavy flavors at the quark level and is uniquely sensitive to neutrino couplings of potential FCNC mediators. All searches are consistent with zero, and limits on the effective mixing strengths $|V_{uc}|^2$, $|V_{db}|^2$, and $|V_{sb}|^2$ are obtained.

I. INTRODUCTION

Flavor-changing neutral current (FCNC) interactions of c - and b -quarks appear in a number of extensions to the Standard Model (SM) of particle physics including extra quark generations [?,?], technicolor [?,?,?,?], multiple Higgs sectors (as in supersymmetry) [?,?,?,?], left-right symmetric models [?], and leptoquarks [?,?]. Evidence for FCNC effects in the heavy quark sector beyond higher order SM processes has not yet been observed. Present limits on FCNC result from searches for rare decays of charm [?] and beauty mesons [?,?,?], in particular decays of the type $D \rightarrow \ell^+ \ell^- X$ and $B \rightarrow \ell^+ \ell^- X$, where $\ell = e$ or μ , $D = (D^+, D^0, D_S^+)$, $B = (B^+, B^0, B_S^0)$; and X is nothing, a pseudoscalar, or a vector meson. The $c \rightarrow u$ transitions are particularly sensitive to new physics since loop level SM-FCNC decays are severely suppressed by the Cabibbo-Kobayashi-Maskawa (CKM) matrix. While experimental signatures for FCNC in D and B decays are clear, their interpretation is ambiguous. Meson decay rates depend on one or more incalculable hadronic form factors. In addition, experimentally attractive final states such as $D^0 \rightarrow e^+ e^-$ and $B^0 \rightarrow \mu^+ \mu^-$ are helicity-suppressed, which obscures dynamical roles played by particular FCNC models.

This article presents an alternative search for FCNC processes in the DIS data of the NuTeV experiment; where either neutrinos or anti-neutrinos interact with a massive iron target. Flavor changing effects can be sought in the reactions

$$\nu_\mu N \rightarrow \nu_\mu c X, \quad c \rightarrow \mu^+ X', \quad (1)$$

$$\nu_\mu N \rightarrow \nu_\mu \bar{b} X, \quad \bar{b} \rightarrow \mu^+ X', \quad (2)$$

$$\nu_\mu N \rightarrow \nu_\mu b X, \quad b \rightarrow c X', \quad c \rightarrow \mu^+ X'', \quad (3)$$

and their charge-conjugates. The experimental signature in the detector is a muon of opposite lepton number from the beam neutrino. It is possible to isolate this final state because NuTeV ran with a high purity sign-selected beam in which the $\bar{\nu}_\mu/\nu_\mu$ event ratio in neutrino mode and the $\nu_\mu/\bar{\nu}_\mu$ ratio in anti-neutrino mode were 0.8×10^{-3} and 4.8×10^{-3} , respectively. Because of the semi-inclusive character of the measurement, FCNC effects in neutrino scat-

tering can be probed at the quark, rather than the hadron level. Furthermore, neutrino scattering is particularly sensitive to any FCNC process mediated by an intermediate neutral object that couples more strongly to neutrinos than to charged leptons (e.g., a Z^0 -like coupling).

II. EXPERIMENTAL APPARATUS AND BEAM

The NuTeV (Fermilab-E815) neutrino experiment collected data during the 1996-97 fixed target run with the refurbished Lab E neutrino detector and a newly installed Sign-Selected Quadrupole Train (SSQT) neutrino beamline. The sign-selection optics of the SSQT pick the charge of secondary pions and kaons which determines whether ν_μ or $\bar{\nu}_\mu$ are predominantly produced. During NuTeV's run the primary production target received 1.13×10^{18} and 1.41×10^{18} protons-on-target in neutrino and anti-neutrino modes, respectively. The SSQT and its performance are described in detail elsewhere [?].

The Lab E detector [?], consists of two major parts; a target calorimeter and an iron toroid spectrometer. The target calorimeter contains 690 tons of steel sampled at 10 cm intervals by 84 3m \times 3m scintillator counters and at 20 cm intervals by 42 3m \times 3m drift chambers. The toroid spectrometer consists of four stations of drift chambers separated by iron toroid magnets. Precision hadron and muon calibration beams monitored the calorimeter and spectrometer performance throughout the course of data taking. The calorimeter achieves a sampling-dominated hadronic energy resolution of $\sigma_{E_{HAD}}/E_{HAD} = 2.4\% \oplus 87\%/\sqrt{E_{HAD}}$ and an absolute scale uncertainty of $\delta E_{HAD}/E_{HAD} = 0.5\%$. The spectrometer's multiple Coulomb scattering dominated muon energy resolution is $\sigma_{E_\mu}/E_\mu = 11\%$ and the muon momentum scale is known to $\delta E_\mu/E_\mu = 1.0\%$. With the selection criteria used in this analysis, the muon charge mis-identification probability in the spectrometer is 2×10^{-5} . This latter rate is confirmed by measurement the muon calibration beam.

III. ANALYSIS PROCEDURE

A. Introduction and Data Selection

The analysis technique consists of comparing the distributions of $y_{VIS} = E_{HAD}/(E_{HAD} + E_{\mu})$ measured in the ν_{μ} and $\bar{\nu}_{\mu}$ wrong sign muon (WSM) data samples to a Monte Carlo(MC) simulation containing all known conventional WSM sources and a possible FCNC signal. The FCNC signal peaks at high y_{VIS} because the decay muon from the heavy flavor hadron is usually much less energetic than the hadron energy produced in the NC interaction. The largest backgrounds, from beam impurities, are concentrated at low y_{VIS} in ν_{μ} and distributed evenly across y_{VIS} in $\bar{\nu}_{\mu}$ mode due to the respective $(1 - y)^2$ and uniform-in- y characteristics of the CC interactions of wrong-flavor beam backgrounds.

Events in the WSM sample must satisfy a number of selection criteria(“cuts”). The fiducial volume cut requires that event vertices be reconstructed at least 25 cm-Fe (cm of iron-equivalent) from the outer edges of the detector in the transverse directions, at least 35 cm-Fe downstream of the upstream face of the detector, and at least 200 cm-Fe upstream of the toroid. Events must possess a hadronic energy of at least 10 GeV, and exactly one track (the muon) must be found. The muon is required to be well-reconstructed and to pass within the understood regions of the toroid’s magnetic field. The muon’s energy must be between 10 and 150 GeV, and its charge must be consistent with having the opposite lepton number as the primary beam component. Requiring that the muon energy reconstructed in different longitudinal sections of the toroid agree within 25% of the value measured using the full toroid reduces charge mis-identification backgrounds to the 2×10^{-5} level. Finally, for the purposes of the final FCNC fit, the reconstructed y_{VIS} is required to be larger than 0.5. With these cuts there are 207 ν -mode and 127 $\bar{\nu}$ -mode WSM events remaining in NuTeV’s nearly 2 million single muon sample.

B. Source and Background Simulations

Conventional WSM sources arise from beam impurities, right-flavor charged current (CC) events where the charge of the muon is mis-reconstructed, CC and NC events where a π or K decays in the hadron shower, charged current (CC) charm production where the primary muon is not reconstructed or the charm quark is produced via a ν_e interaction, and neutral current (NC) $c\bar{c}$ pair production. Single charm CC production and NC $c\bar{c}$ pair production background sources produce broad peaks at high y_{VIS} and must be handled with care. Table ?? gives the fractional contribution of each background component. The relatively large beam impurity background consists of contributions from hadrons (including charm) that decay before the sign-selecting dipoles in the SSQT, neutral kaon decays, muon decays, decay of hadrons produced by secondary interactions in the SSQT (“scraping”), and from decay of wrong-sign pions produced in kaon decays. Table ?? summarizes the relative contributions of each beam source.

A complete GEANT [?] simulation of the SSQT is used to model beam impurities. This simulation uses Malensek’s [?,?] parameterization for hadron production from the primary target. Scraping contributions are modeled by GHEISHA [?]. Production of K_L^0 is handled by extending Malensek’s charged kaon parameterizations using the quark counting relation $K_L^0 = (3K^- + K^+)/4$. Charm production is parametrized using available data from 800 GeV proton beams [?,?]. GEANT properly handles cascade decays such as $K^\pm \rightarrow \pi^\pm \pi^\pm \pi^\mp$, $\pi^\mp \rightarrow \mu^\mp \bar{\nu}_\mu(\nu_\mu)$ and $\pi^\pm \rightarrow \mu^\pm \bar{\nu}_\mu(\nu_\mu)$, $\mu^\pm \rightarrow e^\pm \bar{\nu}_\mu(\nu_\mu) \nu_e(\bar{\nu}_e)$. The NuTeV detector is likewise modeled with a GEANT-based hit-level MC simulation. Wrong-sign muons generated from the flux simulation are propagated through the detector MC and then reconstructed using the same package that is used for data reconstruction. A fast parametric MC is also used to compare the high statistics right-sign flux simulation to data in ν_μ and $\bar{\nu}_\mu$. These comparisons showed that the SSQT dipoles required a downward shift of -2.5% from their nominal values. The right-sign comparisons after these shifts, are shown in Fig. ?? and indicate agreement between predicted flux and data at roughly the 2% level.

The high density target-calorimeter suppresses WSM contributions from π/K decay in the hadron shower; their contribution is estimated from a previous measurement of μ -production in hadron showers using the same detector [?]. The small charge misidentification contribution is estimated by passing a large sample of simulated events through the full detector MC and event reconstruction.

After impurities, the next largest WSM source comes from CC production of charm in which the charm quark decays semi-muonically (dimuon) and its decay muon is picked up in the spectrometer while the primary lepton is either an electron or a muon which exits from or ranges out in the calorimeter. The ν_e beam fraction is 1.9(1.3)% in ν ($\bar{\nu}$)-mode, and 22% of the CC charm events which pass WSM cuts originate from a ν_e . The CC charm background is simulated using a leading-order QCD charm production model with production, fragmentation, and charm decay parameters tuned on neutrino dimuon data collected by NuTeV [?] and a previous experiment using the same detector [?]. Overall normalization of the source is obtained from the measured charm-to-total CC cross section ratio and the single muon right-sign data sample. Simulated dimuon events are passed through the full GEANT simulation of the detector. Fig. ?? provides a check of the modeling of this source through a comparison of the distribution of $y'_{VIS} = E_{HAD}/(E_{HAD} + E_{\mu 2})$, where $E_{\mu 2}$ is the energy of the WSM in the event, between data and MC for dimuon events in which both muons are reconstructed by the spectrometer. This distribution should closely mimic the expected background to the y_{VIS} distribution in the WSM sample. A χ^2 comparison test between data and model yields a value of 19 for 17 degrees of freedom.

Finally, NC $c\bar{c}$ production produces a WSM when the $c(\bar{c})$ decays semi-muonically in $\nu_\mu(\bar{\nu}_\mu)$ mode. An excess over other sources at high y_{VIS} indicates that this source is present in the data; its analysis [?] will appear in a forthcoming publication. For the FCNC search, NC charm production is simulated at production level by a Z^0 -gluon fusion model [?] with charm mass parameter $m_c = 1.70 \pm 0.19$ GeV/ c^2 taken from a next-to-leading (NLO) order QCD analysis of CC charm production [?] and using the GRV94HO [?] gluon parton distribution function (PDF). The NLO charm mass is used because it is influenced in part

by contributions from W –gluon fusion diagrams similar to the Z^0 –gluon process. Note that the value of m_c used is larger than that obtained in LO analyses of CC charm production. This choice tends to reduce the NC charm contribution to the WSM sample and results in more conservative limits on FCNC production. The NC charm quarks are fragmented and decayed using procedures adapted from the CC charm simulation, and the resulting WSM events are then simulated with the full MC.

IV. RESULTS AND INTERPRETATION

A. FCNC Production

The neutrino FCNC $u \rightarrow c$ cross section can be parameterized to LO in QCD as

$$\frac{d\sigma(\nu_\mu u \rightarrow \nu_\mu c; c \rightarrow \mu^+)}{d\xi dy} = \left| \frac{V_{uc}}{V_{cd}} \right|^2 \left[\cos^2 \beta + \sin^2 \beta \frac{(1-y)(1-xy/\xi)}{1-y+xy/\xi} \right] \frac{d\sigma(\nu_\mu d \rightarrow \nu_\mu^- c; c \rightarrow \mu^+)}{d\xi dy}. \quad (4)$$

Here V_{cd} is the $c \rightarrow d$ CKM matrix element, V_{uc} ¹ represents a possible $u \rightarrow c$ coupling, $\sin^2 \beta$ gives the fraction of right-handed coupling of the c –quark to the FCNC, y is the inelasticity, and $\xi \simeq x(1 + m_c^2/Q^2)$ is the fraction of the nucleon’s momentum carried by the struck u –quark, with x the Bjorken scaling variable, Q^2 the squared momentum transfer, and m_c the effective charm quark mass. The $d \rightarrow c$ charged current cross section $d\sigma(\nu_\mu d \rightarrow \nu_\mu^- c; c \rightarrow \mu^+)/d\xi dy$ is measured in the same experiment [?,?]. Since the u and d quark distributions are identical in an isoscalar target, the FCNC cross section should experience the same charm mass suppression as the analogous CC charm production. Fragmentation of subsequent semi-muonic decays of charmed mesons should also be identical for

¹We use the notation V_{uc} , V_{bd} , and V_{sd} in simple analogy to the CKM matrix in order to compare our results to those from FCNC decay searches.. We do not assume any constraints exist for this FCNC CKM-like matrix. In our notation, the FCNC left and right-handed couplings for charm are $g_L^2 = |V_{uc}|^2 \cos^2 \beta$ and $g_R^2 = |V_{uc}|^2 \sin^2 \beta$.

FCNC and CC-charm production. One therefore expects the extracted V_{uc} to have little model dependence.

For FCNC bottom production there is as yet no measured CC analog final state. Therefore, the explicit LO QCD cross section,

$$\frac{d\sigma\left(\nu_\mu N \rightarrow \nu_\mu \bar{b} X\right)}{d\xi' dy} = \frac{G_F^2 M E |V_{bd}|^2}{\pi} \left[\cos^2 \beta' (1-y) (1-xy/\xi) + \sin^2 \beta' (1-y+xy/\xi) \right] \quad (5)$$

$$\times \left(\bar{u}(\xi', Q^2) + \bar{d}(\xi', Q^2) \right),$$

where M is the nucleon mass and E is the neutrino energy, must be convolved with b -quark fragmentation functions for mesons of type B_i (D_b^i) and B_i meson decay distribution functions (Δ_B^i) multiplied by appropriate branching fractions (F_B^i) to yield a WSM cross section:

$$\frac{d\sigma\left(\nu_\mu N \rightarrow \nu_\mu \bar{b}; \bar{b} \rightarrow \mu^+\right)}{d\xi' dy} = \sum_i \frac{d\sigma\left(\nu_\mu N \rightarrow \nu_\mu \bar{b} X\right) \otimes F_B^i D_b^i \otimes \Delta_B^i}{d\xi' dy}. \quad (6)$$

The struck quark momentum fraction ξ' becomes $\xi' \simeq x(1 + m_b^2/Q^2)$, with $m_b = 4.8 \text{ GeV}/c^2$ the effective b -quark mass. It is also possible for FCNC b -production to form a WSM muon signal through the cascade $b \rightarrow c \rightarrow \mu^+$. This mode offers the advantages of the larger and higher ξ valence d -quark PDF at the cost of reduced acceptance for the softer c -decay muon. A similar expression holds for FCNC $s \rightarrow b$ transitions with the replacements $u(\xi', Q^2) + d(\xi', Q^2) \rightarrow 2s(\xi', Q^2)$, $|V_{bd}|^2 \rightarrow |V_{bs}|^2$, and $\sin^2 \beta' \rightarrow \sin^2 \beta''$.

Production cross sections for both c - and b - FCNC sources are computed from the GRV94LO PDF set [?] for several choices of right-left coupling admixtures. Acceptance for a charm FCNC-WSM signal is calculated using a fragmentation-decay model tuned to NuTeV and CCFR dimuon data [?]. For FCNC-WSM from b -quarks, fragmentation and decays are handled with the Lund string fragmentation model [?]. Detector response is simulated with the full hit-level MC.

B. Fits to Data

Binned likelihood fits are performed to the y_{VIS} distributions of the data using a model consisting of all conventional WSM sources described above and an FCNC source. The fit varies the level, but not the shape, of the FCNC signal contribution. The NC charm contribution is also varied in shape and level by allowing m_c to float within its errors. The three FCNC sources ($u \rightarrow c$, $d \rightarrow b$, and $s \rightarrow b$) are treated separately. Only neutrino data is used for the $u \rightarrow c$, but both modes are used for FCNC bottom production to exploit the possibility of a cascade decays to charm. A series of fits are performed for each FCNC source, corresponding to different mixtures of right and left-handed FCNC couplings to the quarks; a typical result is shown in Fig. ??.

In all cases, the signal for FCNC is within $\pm 2.0 \sigma$ of zero, and limits are set accordingly. Since Gaussian statistics apply, the 90% confidence level upper limit is set by adding 1.64σ to the best-fit value if the best-fit value is positive, or 1.64σ to zero if the best fit is negative. Here, σ consists of the statistical error from the fit added in quadrature to the estimated systematic error described in the next section. Table ?? summarizes the fit results.

C. Systematic Errors

The dominant systematic errors result from modeling the rejection of CC charm events, and the overall normalization of CC charm events. Estimates of systematic uncertainties are obtained by varying the event selection procedure as well as parameters characterizing the detector response and physics models. Errors are assumed to be independent.

Charged current charm events are removed by requiring that exactly one track be found and reconstructed by the NuTeV tracking software. Another independent way to remove dimuons is to use calorimeter information. The *stop* parameter is the first of three consecutive counters downstream of the interaction, each with less than 1.5 MIPs. The *stop* cut requires that the distance between the interaction and the *stop* counter be less than 15

counters. Replacing the tracking cut with the *stop* cut gives the systematic errors listed in Table ??.

The next largest systematic error is due to the normalization of CC charm events. Normalization of these events is obtained from the right-sign muon CC sample. One can also normalize CC charm events with only one reconstructed track, to those with both tracks found. These normalizations disagree by 3% resulting in the systematic errors listed in Table ?. Systematic errors due to the beam normalization, detector calibration, and other sources are small.

D. Comparison to Limits from Decays

For comparison purposes, the following expressions are used to relate FCNC heavy flavor meson decay branching fractions (BF) to the parameter V_{uc} :

$$BF(D^0 \rightarrow \ell^+ \ell^-) = 2 \left| \frac{V_{uc}}{V_{cs}} \right|^2 \frac{m_\ell^2}{m_\mu^2} BF(D_S^+ \rightarrow \mu^+ \nu_\mu), \quad (7)$$

$$BF(D^+ \rightarrow \pi^+ \ell^+ \ell^-) = \left| \frac{V_{uc}}{V_{cd}} \right|^2 BF(D^+ \rightarrow \pi^+ \ell^+ \nu_\ell), \quad (8)$$

$$BF(D_S^+ \rightarrow K^+ \ell^+ \ell^-) = \left| \frac{V_{uc}}{V_{cs}} \right|^2 BF(D_S^+ \rightarrow \eta \ell^+ \nu_\ell). \quad (9)$$

For estimates of V_{db} and V_{sb} from B decays, it is assumed that

$$BF(B^0 \rightarrow \ell^+ \ell^-) = 2 \left| \frac{V_{bd}}{V_{ub}} \right|^2 \frac{m_\ell^2}{m_\mu^2} BF(B^+ \rightarrow \mu^+ \nu_\mu), \quad (10)$$

$$BF(B^+ \rightarrow \pi^+ \ell^+ \ell^-) = \left| \frac{V_{bd}}{V_{ub}} \right|^2 BF(B^0 \rightarrow \pi^- \ell^+ \nu_\ell), \quad (11)$$

$$BF(B_s^0 \rightarrow \ell^+ \ell^-) = 2 \left| \frac{V_{bs}}{V_{ub}} \right|^2 \frac{m_\ell^2}{m_\mu^2} BF(B^+ \rightarrow \mu^+ \nu_\mu), \quad (12)$$

$$BF(B^+ \rightarrow K^+ \ell^+ \ell^-) = \left| \frac{V_{bs}}{V_{cb}} \right|^2 BF(B^+ \rightarrow D^0 \ell^+ \nu_\ell). \quad (13)$$

Measured values [?] are used for the branching fractions on the right hand side except for the leptonic decay $B^+ \rightarrow \mu^+ \nu_\mu$, for which it is assumed that

$$BF(B^+ \rightarrow \mu^+ \nu_\mu) = 2.2 \times 10^{-6} (f_B/200 \text{ MeV})^2, \quad (14)$$

with $f_B = 200$ MeV, the B decay constant.

Table ?? summarizes the limits on $|V_{uc}|^2$, $|V_{bd}|^2$, and $|V_{sb}|^2$ from meson decays. We note that our overall limits from neutrino scattering, which would approximately correspond to decay searches of the type $D \rightarrow \nu_\mu \bar{\nu}_\mu X$ and $B \rightarrow \nu_\mu \bar{\nu}_\mu X$, are generally weaker than the decay search limits. Our result for V_{db} is competitive, and we have effectively added new modes to the search that do not depend on specific mechanisms for heavy meson decay.

V. CONCLUSION

In this paper we have established a new method for probing FCNC processes in deep inelastic neutrino scattering. Our experiment tests for FCNC at the inclusive quark level, and we are particularly sensitive to any FCNC process in which the mediating field couples more strongly to neutrinos than to charged leptons. We observe no evidence for FCNC interactions, and we set limits on the effective mixing elements $|V_{uc}|^2$, $|V_{bd}|^2$, and $|V_{bs}|^2$ at the 10^{-3} level.

ACKNOWLEDGMENTS

We would like to thank the staffs of the Fermilab Particle Physics and Beams Divisions for their contributions to the construction and operation of the NuTeV beamlines. We would also like to thank the staffs of our home institutions for their help throughout the running and analysis of NuTeV. This work has been supported by the U.S. Department of Energy and the National Science Foundation.

REFERENCES

- [1] V. Barger, M.S. Berger, and R.J.N. Phillips, Phys. Rev. **D53** (1995)1663.
- [2] K. S. Babu, *et al.*, Phys. Lett. **B205** (1988) 540.
- [3] S. Dimopolous, H. Georgi, and S. Raby, Phys. Lett. **B127** (1983) 101.
- [4] V.A. Miransky, S. Peris, and S. Raby, Phys. Rev. **D47** (1993) 2058.
- [5] C.D. Carone and R.T. Hamilton, Phys. Lett. **B301** (1993) 162.
- [6] E. Eichten and K. Lane, Phys. Lett. **B90** (1980) 125.
- [7] R.S. Chikula, H. Georgi, and L. Randall, Nucl. Phys. **B292** (1987) 93.
- [8] M. Luke and M.J. Savage, Phys. Lett. **B307** (1993) 387.
- [9] J. L. Diaz-Cruz and G.L. Castro, Phys. Lett. **B301** (1993) 405.
- [10] K. Koike, Prog. Theor. Phys. **91** (1994) 161.
- [11] J. G. Koner, A. Pilaftsis, and K. Schilcher, Phys. Rev. **D47** (1994) 1080.
- [12] F. J. Gilman, K. Kleinknecht, and B. Renk, Phys. Rev. **D50** (1994) 1315.
- [13] W. Buchmuller, D. Wyler, Phys. Lett. **B177** (1986) 377.
- [14] S. Davidson, D. Bailey, and B.A. Campbell, Z. Phys. **C61** (1994) 313.
- [15] E.M. Aitala *et al.* (Fermilab E791 Collaboration), Phys. Lett. **B462** (1999) 401.
- [16] T. Affolder, “Search for the Flavor-Changing Neutral Current Decays $B^+ \rightarrow \mu^+ \mu^- K^+$ and $B^0 \rightarrow \mu^+ \mu^- K^{*0}$ ”, hep-ex/9905004.
- [17] F. Abe *et al.* [CDF Collaboration], Phys. Rev. **D57**, 3811 (1998).
- [18] A. Weir, Phys. Rev. **D41**, 1384 (1990)
- [19] C. Caso *et al.*, Eur. Phys. J. **C3**, 1 (1998).

- [20] M. Gluck, E. Reya, and A. Vogt, Z. Phys. **C67**, 433 (1995).
- [21] NuTeV Collaboration, J. Yu, *et al.*, Report No. FERMILAB-TM-2040, 1998.
- [22] D. A. Harris *et al.* [NuTeV Collaboration], Nucl. Instrum. Meth. **A447**, 377 (2000) [hep-ex/9908056]. B. King, *et al.*, *ibid.* 302, 254 (1991).
- [23] M. Gluck, R. M. Godbole, and E. Reya, Z. Phys. **C38**, 441 (1988).
- [24] CERN CN/ASD, “GEANT Detector Description and Simulation Library” (1998).
- [25] A.J. Malensek, “Empirical Formula For Thick Target Particle Production,” FERMILAB-FN-0341.
- [26] H. W. Atherton *et al.*, CERN-80-07.
- [27] H. Fesefeldt, PITHA-85-02.
- [28] R. Ammar *et al.*, Phys. Rev. Lett. **61**, 2185 (1988).
- [29] K. Kodama *et al.* [Fermilab E653 Collaboration], Phys. Lett. **B263**, 573 (1991).
- [30] M. Goncharov *et al.*, to be published in *Proceedings of the 34th Rencontres de Moriond, QCD and Hadronic Interactions* (2000).
- [31] B. Anderson *et al.*, Phys. Rep. **97**, 1983.
- [32] P. Sandler, Ph.D. Thesis, Univ. of Wisconsin, 1992.
- [33] A. Alton, Ph.D. Thesis, Kansas State University, 2000.
- [34] A.O. Bazarko *et al.* [CCFR Collaboration], Z. Phys. **C65**, 189 (1995)
- [35] N. Witchey, Ph.D. Thesis, Ohio State University, 1996.
- [36] R. Ammar *et al.* [CLEO Collaboration], Phys. Rev. **D49**, 5701 (1994).
- [37] P. Avery *et al.* [CLEO Collaboration], Phys. Lett. **B183**, 429 (1987).

[38] M. Acciarri *et al.* [L3 Collaboration], Phys. Lett. **B391**, 474 (1997).

FIGURES

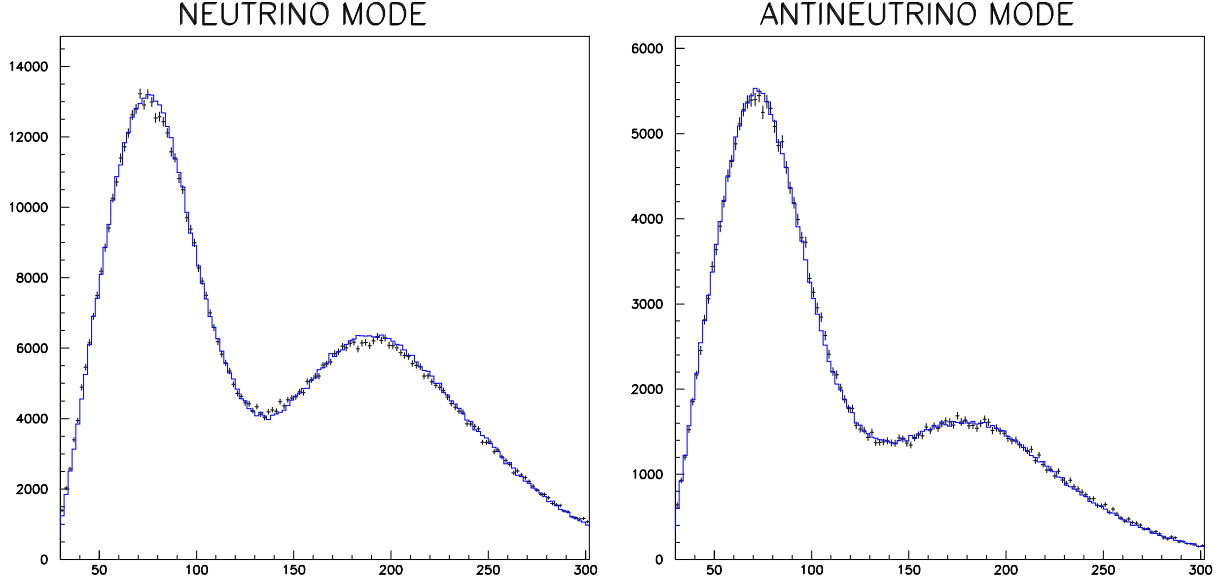


FIG. 1. Comparison of ν and $\bar{\nu}$ CC energy spectrum for data (pluses) to MC(histogram) using the GEANT-based flux.

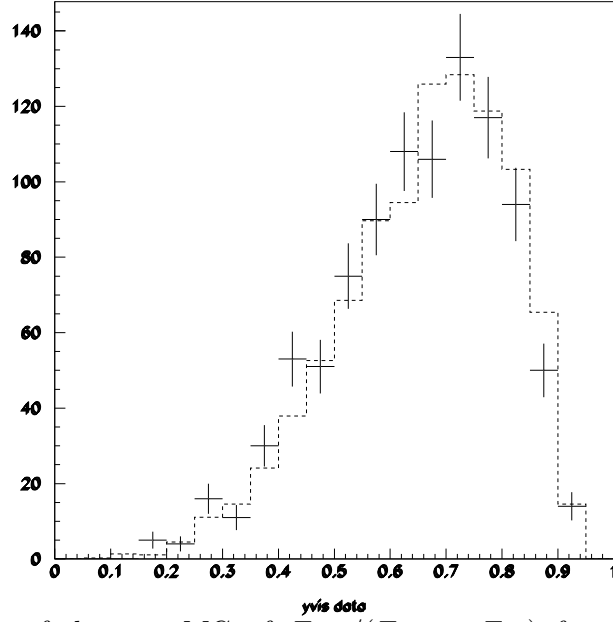


FIG. 2. Comparison of data to MC of $E_{had}/(E_{had} + E_{\mu 2})$ for dimuon events with two toroid-analyzed muons.

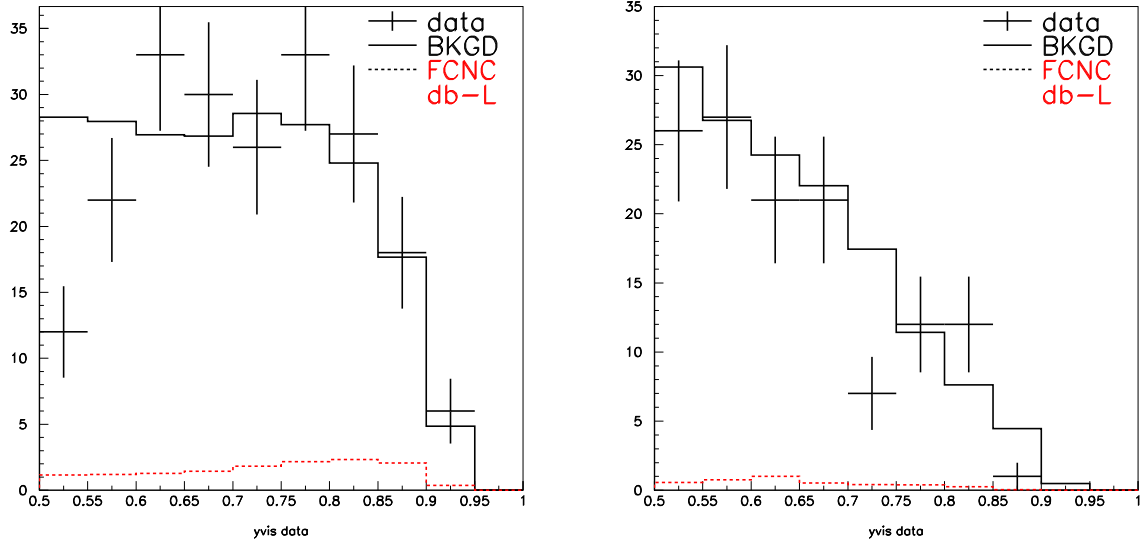


FIG. 3. Comparison of y_{VIS} distributions of data (pluses) to predictions of all Standard Model sources (solid) of WSM's and the FCNC signal(dashed). The plot on the left is neutrino mode, while that on the right is anti-neutrino mode.

TABLES

Source	ν -mode(%)	$\bar{\nu}$ -mode(%)
Beam Impurity	67	83
Charged Current Charm	19	8
Charge Misidentification	5	5
Neutral Current Charm	5	2
Neutral Current π/K decay	2	1
Charged Current π/K decay	1	1

TABLE I. Percentage of WSM's for each source in a given mode.

	ν -mode	$\bar{\nu}$ -mode
	$E\nu > 20$ GeV	$E\nu > 20$ GeV
scraping	53%	24%
charm	10%	25%
K^0	12%	16%
other prompt	9%	22%
muon decay	11%	11%
$K \rightarrow \pi \rightarrow \mu$	5%	2%

TABLE II. The percentage of beam impurities due to a given source in each mode.

Transition	$\sin^2 \beta$	V^2	Limit
$u \rightarrow c$	0.0	$(1.1 \pm 1.5 \pm 0.5) \times 10^{-3}$	3.7×10^{-3}
	0.10	$(1.2 \pm 1.7 \pm 0.9) \times 10^{-3}$	4.4×10^{-3}
	0.35	$(1.6 \pm 2.2 \pm 2.6) \times 10^{-3}$	7.2×10^{-3}
	0.65	$(2.5 \pm 3.6 \pm 5.4) \times 10^{-3}$	13.1×10^{-3}
	0.90	$(4.1 \pm 7.9 \pm 7.9) \times 10^{-3}$	22.4×10^{-3}
	1.00	$(4.4 \pm 13.7 \pm 8.7) \times 10^{-3}$	34.5×10^{-3}
$d \rightarrow b$	0.00	$(.3 \pm 1.3 \pm 0.7) \times 10^{-3}$	2.7×10^{-3}
	0.10	$(-0.15 \pm 1.2 \pm 0.7) \times 10^{-3}$	2.3×10^{-3}
	0.35	$(-1.2 \pm 1.2 \pm 0.7) \times 10^{-3}$	2.2×10^{-3}
	0.65	$(-1.6 \pm 0.90 \pm 0.6) \times 10^{-3}$	1.8×10^{-3}
	0.90	$(-1.4 \pm 0.79 \pm 0.6) \times 10^{-3}$	1.6×10^{-3}
	1.00	$(-1.3 \pm 0.68 \pm 0.6) \times 10^{-3}$	1.5×10^{-3}
$s \rightarrow b$	0.0	$(-17.3 \pm 17.3 \pm 3.51) \times 10^{-3}$	29×10^{-3}
	0.10	$(-13.6 \pm 6.6 \pm 3.3) \times 10^{-3}$	12×10^{-3}
	0.35	$(-3.6 \pm 1.9 \pm 2.7) \times 10^{-3}$	5.4×10^{-3}
	0.65	$(-1.9 \pm 1.0 \pm 2.0) \times 10^{-3}$	3.7×10^{-3}
	0.90	$(-1.4 \pm 0.7 \pm 1.5) \times 10^{-3}$	2.7×10^{-3}
	1.00	$(-1.3 \pm 0.7 \pm 1.2) \times 10^{-3}$	2.3×10^{-3}

TABLE III. Results of the FCNC fits.

Transition	Coupling	Dimuon Rejection	Dimuon Normalization	Energy	Beam	Total
$u \rightarrow c$	L	0.30×10^{-3}	0.32×10^{-3}	0.23×10^{-3}	0.01×10^{-3}	0.50×10^{-3}
$u \rightarrow c$	R	8.08×10^{-3}	3.22×10^{-3}	0.24×10^{-3}	0.02×10^{-3}	8.70×10^{-3}
$d \rightarrow b$	L	0.36×10^{-3}	0.22×10^{-3}	0.51×10^{-3}	0.14×10^{-3}	0.68×10^{-3}
$d \rightarrow b$	R	0.25×10^{-3}	0.10×10^{-3}	0.04×10^{-3}	0.55×10^{-3}	0.61×10^{-3}
$s \rightarrow b$	L	2.37×10^{-3}	0.21×10^{-3}	0.91×10^{-3}	2.42×10^{-2}	3.51×10^{-2}
$s \rightarrow b$	R	1.08×10^{-3}	0.06×10^{-3}	0.20×10^{-3}	0.54×10^{-2}	1.22×10^{-2}

TABLE IV. Table of systematic errors on FCNC results. “L” refers to pure left-handed coupling ($\sin^2 \beta = 0$), while “R” refers to pure right-handed coupling ($\sin^2 \beta = 1$).

FCNC	BF	Allowed	$ V ^2$	Limit with	
decay	Limit	Decay	limit	BR error	reference
$D^\pm \rightarrow \pi^\pm \mu^\pm \mu^\mp$	1.7×10^{-5}	$D^\pm \rightarrow \pi^0 l^\pm \nu_l$	2.3×10^{-4}	2.7×10^{-4}	[?]
$B^\pm \rightarrow \pi^\pm e^\pm e^\mp$	3.9×10^{-3}	$B^0 \rightarrow \pi^0 l^\pm \nu_l$	1.6×10^{-3}	2.1×10^{-3}	[?]
$B^\pm \rightarrow K^\pm e^\pm e^\mp$	3.9×10^{-5}	$B^0 \rightarrow D^0 l^\pm \nu_l$	2.4×10^{-5}	2.1×10^{-5}	[?]

TABLE V. Limits on FCNC couplings from meson decay searches, with $|V|^2 = |V_{uc}|^2, |V_{db}|^2$, or $|V_{sb}|^2$ as appropriate. Equations ??-?? relate branching fraction(BF) limits to the $|V|^2$ limits in the table.